

# On the link between intrinsic catalytic reactions kinetics and the development of catalytic processes

## Catalytic dehydrogenation of ethylbenzene to styrene

S.S.E.H. Elnashaie<sup>a,\*</sup>, B.K. Abdallah<sup>b</sup>, S.S. Elshishini<sup>c</sup>, S. Alkhowaiter<sup>d</sup>,  
M.B. Noureldeen<sup>a</sup>, T. Alsoudani<sup>e</sup>

<sup>a</sup> Department of Chemical Engineering, Auburn University, Auburn, AL 36849, USA

<sup>b</sup> Department of Chemical Engineering, Qatar University, Al-Doha, Qatar

<sup>c</sup> Department of Chemical Engineering, Cairo University, Cairo, Egypt

<sup>d</sup> Department of Chemical Engineering, Petrochemical and Petroleum Refining Institute (PAPRI), King Abdulaziz City for Science and Technology (KACST), Riyadh, Saudi Arabia

<sup>e</sup> Department of Chemical Engineering, KFUPM, Dhahran 31261, Saudi Arabia

### Abstract

A procedure linking kinetic modeling of catalytic reactions to reactor modeling for different configurations is developed and applied to the catalytic dehydrogenation of ethylbenzene to styrene. The procedure is applied to four configurations, namely fixed bed with/without hydrogen selective membranes and bubbling fluidized beds with/without selective membranes. The kinetic data for the industrial catalyst are extracted from industrial fixed bed data using a rigorous heterogeneous model. The kinetic data for the three in-house prepared catalysts are obtained from the laboratory scale experiments using pseudo-homogeneous models. © 2001 Elsevier Science B.V. All rights reserved.

**Keywords:** Catalytic dehydrogenation; Ethylbenzene; Intrinsic kinetics; Fixed/fluidized bed reactors; Membrane catalytic reactors

### 1. Introduction

The usual catalyst evaluation procedure in a laboratory differential/integral fixed bed reactor based on comparing different catalysts on the basis of their activity (conversion) and yield of desired product (selectivity)

does not give enough information about the catalyst behavior for the development of the commercial catalytic processes. The evaluation of the catalysts according to this simple and fast procedure may change when the catalysts are used in the commercial/pilot scale units of different configurations due to a number of factors, which are not accounted for in the laboratory experiments, the main factors are the following:

1. interphase/intraparticle diffusional resistances;
2. variation of the mixture composition in different sections of the unit;
3. the specific configuration of the unit.

A more comprehensive approach that combines kinetic and reactor modeling for catalytic processes,

*Abbreviations:* BZ, EB, H<sub>2</sub>, ST, TOL, benzene, ethylbenzene, hydrogen, styrene, toluene; BD, bubble to dense (emulsion) phase; D, dense (emulsion) phase; B, bubble phase; F, feed; X<sub>EB</sub>, total conversion of ethylbenzene; Y<sub>BZ</sub>, Y<sub>ST</sub>, Y<sub>TOL</sub>, yield of benzene, styrene and toluene

\*Corresponding author. Tel.: +1-334-887-3904; fax: +1-334-887-3905.

E-mail addresses: nashaie@eng.auburn.edu, elnashaie@hotmail.com (S.S.E.H. Elnashaie).

**Nomenclature**

$A_B, A_D, A_t$	cross-sectional area of bubble phase, dense phase and reactor tube ( $\text{m}^2$ )
$C_0$	molar concentration of $\text{H}_2$ in the membrane ( $\text{kmol}/\text{m}^3$ )
$C_i$	concentration of component $i$ ( $\text{kmol}/\text{m}^3$ )
$C_{pi}, C_{pG}$	heat capacity of component $i$ and of the gas mixture ( $\text{kJ}/\text{kmol}$ )
$d_B, d_p$	bubble and particle diameter (m)
$D_{\text{H}_2}, D_{i,m}$	diffusivity of $\text{H}_2$ through the membrane, binary diffusivity of components $i$ and $m$ ( $\text{m}^2/\text{h}$ )
$G_0$	mass velocity of gas mixture ( $\text{kg}/\text{m}^2 \text{ h}$ )
$(H_{\text{BD}})_B, H$	interphase heat transfer coefficient between bubble and dense phase based on bubble volume ( $\text{kJ}/\text{m}^3 \text{ h K}$ ), total height of fluidized bed (m)
$\Delta H_j, h$	heat of reaction $j$ ( $\text{kJ}/\text{kmol}$ ), height co-ordinate for fluidized bed (m)
$k_i, l$	rate constant of reaction $i$ ( $\text{kmol}/\text{kg-cat h bar}$ ), height co-ordinate of fixed bed (m)
$(K_{\text{BD}})_{iB}$	interphase mass transfer coefficient of component $i$ between bubble and dense phase based on bubble volume ( $\text{l/h}$ )
$K_{\text{EB}}, L$	ethylbenzene equilibrium constant (bar), total height of fixed bed (m)
$N_i$	molar flux of component $i$ ( $\text{kmol}/\text{h}$ )
$p_0$	standard pressure for the permeation side (bar)
$p_{\text{H}_2}$	hydrogen partial pressure in the reactor side (bar)
$p'_{\text{H}_2}$	hydrogen partial pressure in the membrane side (bar)
$P$	total pressure of the reactor (bar)
$P_i$	partial pressure of component $i$ (bar)

$Q_B, Q_D$	volumetric flow rate in bubble phase and dense phase, respectively ( $\text{m}^3/\text{h}$ )
$Q_{\text{H}_2}, r_j, R_i$	molar rate of hydrogen in the membrane tube ( $\text{kmol}/\text{h}$ ), intrinsic rates of reaction $j$ and component $i$ , respectively ( $\text{kmol}/\text{kg-cat h}$ )
$r_p$	radius of catalyst pellet
$T, T_B, T_D$	temperature of reactor, bubble phase and dense phase, respectively (K)
$X_i, y_i$	conversion and mole fraction of component $i$
$z$	catalyst pellet depth co-ordinate

*Greek letters*

$\alpha_{\text{H}_2}$	permeation rate constant of hydrogen through the membrane ( $\text{m}^2/\text{h bar}$ )
$\Gamma_o, \Gamma_i$	outer and inner radii of the permeable tube (m)
$\delta$	bubble phase volume fraction to the total volume of the bed (dimensionless)
$\varepsilon_p, \varepsilon$	catalyst pellet porosity and catalyst bed void fraction, respectively
$\eta_j, \eta_i$	effectiveness factor of reaction $j$ , and component $i$ , respectively
$\mu_g$	gas viscosity ( $\text{kgf h}/\text{m}^2$ )
$\rho_c, \rho_B, \rho_G$	density of catalyst particles, bulk density of catalyst, and of gas mixture ( $\text{kg}/\text{m}^3$ )

consists of the following steps:

1. Utilization of the laboratory reactor results to develop reliable kinetic rate equations for different catalysts.
2. Development of rigorous diffusion–reaction models (e.g. dusty gas models for the catalyst pellets based on the Stefan–Maxwell equations rather than the approximate Fickian diffusion models) for the industrial/pilot scale units.
3. Verification of the models against industrial/pilot plant data, whenever such data are available.

4. Simulation of the behavior of the different catalysts in the different configurations using the verified rigorous models.
5. Evaluation of the different catalysts in relation to the industrial/pilot reactor configuration.
6. Comparison between the different configurations each with its optimal catalyst.

In the present paper, the above approach is illustrated and discussed for the industrially important catalytic dehydrogenation of ethylbenzene to styrene. One of the commercial catalysts is used together with three in-house prepared catalysts with different promoters. The four catalysts are evaluated according to the above procedure for the following configurations: the industrial fixed bed, fixed bed with hydrogen selective composite membranes, fluidized bed with and without selective membranes.

## 2. The reaction network

The reaction network for the dehydrogenation of ethylbenzene to styrene can be represented by the following six reactions: one main reaction for the production of styrene and five side reactions [1,2].

*Main reaction:*



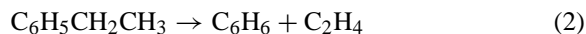
$$r_1 = k_1 \left( \frac{P_{\text{EB}} - P_{\text{ST}} P_{\text{H}_2}}{K_{\text{EB}}} \right)$$

$$K_{\text{EB}} = \exp \left( \frac{-\Delta F^0}{RT} \right)$$

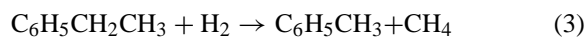
$$\Delta F^0 = a + bT + cT^2$$

where  $a = 122725.16$  (kJ/kmol),  $b = -126.27$  (kJ/kmol K) and  $c = -2.19 \times 10^{-3}$  (kJ/kmol K<sup>2</sup>)

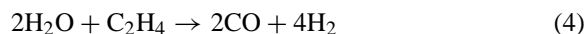
*Side reactions:*



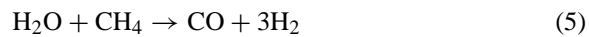
$$r_2 = k_2 P_{\text{EB}}$$



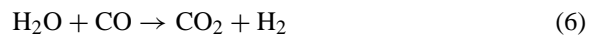
$$r_3 = k_3 P_{\text{EB}} P_{\text{H}_2}$$



$$r_4 = k_4 P_{\text{H}_2\text{O}} P_{\text{ETH}}$$



$$r_5 = k_5 P_{\text{H}_2\text{O}} P_{\text{MET}}$$



$$r_6 = k_6 \left( \frac{P_{\text{T}}}{T^3} \right) P_{\text{H}_2\text{O}} P_{\text{CO}}$$

The intrinsic kinetic rate constants (pre-exponential factors and activation energies) are extracted from industrial fixed bed data using rigorous heterogeneous model. The net rates of ethylbenzene and steam formation are given by the following equations:

$$R_{\text{EB}} = -(r_1 + r_2 + r_3), \quad R_{\text{H}_2\text{O}} = -(r_4 + r_5 + r_6)$$

The rates of formation of the main products are given by the following equations:

$$R_{\text{ST}} = r_1, \quad R_{\text{BZ}} = r_2, \quad R_{\text{TOL}} = r_3$$

The rate of production of hydrogen is given by the equation as follows:

$$R_{\text{H}_2} = r_1 - r_3 - 2r_4 + 3r_5 + r_6$$

Other components can be expressed in a similar manner.

## 3. Model equations

### 3.1. Fixed bed with/without hydrogen selective composite membranes

For the industrial fixed bed reactor, the catalyst packing the reactor is composed of an iron oxide (Fe<sub>2</sub>O<sub>3</sub>) doped with potassium carbonate (K<sub>2</sub>CO<sub>3</sub>) and chromium oxide (Cr<sub>2</sub>O<sub>3</sub>). The catalyst particles are extrudates of cylindrical shape. Since at steady state the problem of simultaneous diffusion and reaction are independent of particle shape; an equivalent slab geometry was used for the catalyst pellet, with a characteristic length giving surface to volume ratio of the slab equal to that of the original shape [3]. The intrapellet mass balance equation is expressed as follows:

$$\frac{dC_i}{dz} = \rho_c R_i \quad (7)$$

where  $R_i$  is the net rate of production of component  $i$ .

The Stefan–Maxwell equation for multicomponent diffusion [4–6] is given by the following equation:

$$-\left(\frac{dC_i}{dz}\right) = \left(\frac{N_i}{D_{kei}}\right) + \sum_{m=1}^M \frac{(y_i N_m - y_m N_i)}{D_{ei,m}} \quad (8)$$

where  $M$  is the total number of components of the system ( $M = 10$ ), effective diffusivities  $D_{ei,m}$  are calculated from molecular diffusivities,  $D_{i,m}$ , catalyst porosity,  $\varepsilon_p$ , and tortuosity,  $\tau$ , with boundary conditions which are as follows:

$$N_i = 0 \quad \text{at } z = 0 \quad (9a)$$

$$C_i(r_p) = C_{is} \quad \text{at } z = r_p \quad (9b)$$

Boundary condition (9b) indicates negligible external mass transfer resistance between the catalyst pellet and the bulk gas. This is a valid assumption for the high gas flow rate in the reactor.

The performance of the pellet is expressed in terms of the effectiveness factors of each reaction and also the effectiveness factors of the components. The effectiveness factors are computed using the following well-known relation (reaction effectiveness factors) for reaction  $j$ :

$$\eta_j = \left(\frac{1}{r_p r_j^s}\right) \int_0^{r_p} r_j dz \quad (10a)$$

The component effectiveness factors are similarly given by the following relation for component  $i$ :

$$\eta_i = \left(\frac{1}{r_p R_i^s}\right) \int_0^{r_p} R_i dz \quad (10b)$$

The global orthogonal collocation technique [7,8] is used for approximating the derivatives and the integrals of the above equations (Eqs. (7), (8) and (10a,b)).

Mass balance differential equations for the bulk gas phase are given by the following equations:

$$\frac{dX_k}{dl} = \frac{\eta_k \rho_B A_t r_k}{F_{EBF}} \quad (11)$$

$$\frac{dX_n}{dl} = \frac{\eta_n \rho_B A_t r_n}{F_{H_2OF}}, \quad X_k = X_n = 0 \text{ at } l = 0 \quad (12)$$

where  $k$  is for reactions (1)–(3) and  $X_k$  the fractional conversion of ethylbenzene in each of these reactions; while  $n$  is for reactions (4)–(6) and  $X_n$  the fractional

Table 1

Industrial fixed reactor specification, catalyst properties and feed conditions

	Symbol	Value	Dimension
Reactor diameter	$D$	1.95	m
Catalyst bed depth	$L$	1.70	m
Catalyst density	$\rho_c$	2146	kg/m <sup>3</sup>
Catalyst diameter	$D$	4.7	mm
Catalyst pore radius	$r_p$	2400	Å
Catalyst porosity	$\varepsilon_p$	0.35	
Catalyst tortuosity	$\tau$	4.0	
Inlet pressure	$P_F$	2.4	bar
Inlet temperature	$T_F$	922.6	K
<i>Inlet gas molar flow rates</i>			
Ethylbenzene	EB	36.87	kmol EB/h
Styrene	ST	0.67	kmol ST/h
Benzene	BZ	0.11	kmol BZ/h
Toluene	TOL	0.88	kmol TOL/h
Steam	H <sub>2</sub> O	453	kmol H <sub>2</sub> O/h
Total molar feed	TMF	491	kmol/h
Total mass flow	TMFR	12238	kg/h

conversion of the steam in each of these reactions. The Ergun equation is used for the pressure drop [9] as follows:

$$\begin{aligned} \frac{dP}{dl} = & - \left[ \frac{10^{-5}(1-\varepsilon)G_0}{(d_p \varepsilon^3 \rho_G g_c)} \right] \\ & \times \left[ 1.75 G_{0+} \frac{150(1-\varepsilon)\mu_G}{d_p} \right], \\ P = P_F \text{ at } l = 0 \end{aligned} \quad (13)$$

These results are not very sensitive to the constants of the Ergun equation because of the small pressure drop along the length of the reactor (see Tables 1 and 2).

The energy balance differential equation is given by

$$\frac{dT}{dl} = \frac{\sum (-\Delta H_j) \eta_j \rho_B r_j A_t}{\sum_{i=1}^{10} F_i C_{p_i}}, \quad T = T_F \text{ at } l = 0 \quad (14)$$

An implicit assumption in the above model equation is that external heat transfer resistance between the catalyst pellets and the bulk gas is negligible due to the high gas flow rate and that intraparticle heat transfer resistance is negligible due to the high thermal conductivity of the catalyst pellets [6].

The permeation rate of hydrogen gas through the palladium membrane  $Q_{H_2}$  is assumed to obey the

Table 2  
Results of the heterogeneous model as compared with the industrial reactor data<sup>a</sup>

	Industrial reactor		Heterogeneous model	
	Molar flow rate (kmol/h)	Conversion and yield (%)	Molar flow rate (kmol/h)	Conversion and yield (%)
<i>Conversion</i>				
EB	19.45	47.26	19.29	47.45
H <sub>2</sub> O			447.32	1.26
<i>Yield</i>				
ST	15.56	40.37	15.53	40.17
BZ	1.5	3.77	1.64	4.12
TOL	2.03	3.12	2.07	3.17
Exit pressure (bar)	2.32		2.38	
Exit temperature (K)	850.0		851.10	

<sup>a</sup> Output water is not measured in plant operation.

half-power pressure law [10].

$$\frac{dQ_{H_2}}{dl} = \alpha_{H_2} \sqrt{\left(\frac{p_{H_2}}{p_0}\right)} - \sqrt{\left(\frac{p'_{H_2}}{p_0}\right)},$$

$$Q_{H_2} = 0 \text{ at } l = 0 \quad (15)$$

where  $\alpha_{H_2}$  is the permeation rate constant of hydrogen given by

$$\alpha_{H_2} = \frac{2\pi D_{H_2} C_0}{\ln(\Gamma_o/\Gamma_i)} \quad (16)$$

with

$$D_{H_2} = 8.28 \times 10^{-4} \exp\left(\frac{-21700}{RT}\right) \quad (17)$$

$$C_0 = 302.97 \times T^{-1.0358} \quad (18)$$

where  $D_{H_2}$  is Fick's diffusion coefficient of hydrogen dissolved in palladium. Palladium tubes can be used, however, other membranes can be more suitable for practical applications to avoid the disadvantages of pure palladium tubes [11]. For the membrane reactors equation (15) is integrated simultaneously with the model equations and the hydrogen flux through the membrane is subtracted from the hydrogen balance at each integration step. For the non-membrane fixed bed, the same model and equations can be used with  $\alpha_{H_2} = 0$ . The pseudo-homogeneous model is obtained by setting all  $\eta_j$ ,  $\eta_i = 1.0$ .

### 3.2. Fluidized bed with/without hydrogen selective membranes

A relatively rigorous model of the bubbling fluidized bed reactor for the dehydrogenation of EB to styrene, with and without selective membranes is developed. The model uses the usual assumptions of: perfectly mixed emulsion (dense) phase, plug-flow bubble phase and negligible solids in the bubble phase. The hydrodynamic and interphase mass and heat transfer parameters are evaluated from well established correlations [12–15].

#### 3.2.1. Mass and energy balances for the bubble phase

Material balance for component  $i$  gives

$$\frac{dN_{iB}}{dh} = A_B(K_{BD})_{iB} \left[ \left(\frac{N_{iD}}{Q_D}\right) - \left(\frac{N_{iB}}{Q_B}\right) \right],$$

$$N_{iB} = N_{iBF} \text{ at } h = 0 \quad (19)$$

Let  $A_B(K_{BD})_{iB}/Q_B = \alpha_i$  then, Eq. (19) is rearranged and integrated to give the molar flow rate profile of components in the bubble phase:

$$N_{iB} = Q_B \left[ \left(\frac{N_{iD}}{Q_D}\right) - \left[ \left(\frac{N_{iD}}{Q_D}\right) - \left(\frac{N_{iBF}}{Q_B}\right) \right] e^{-\alpha_i h} \right] \quad (20)$$

The energy balance of the bubble phase is given by

$$\frac{dT_B}{dh} = \frac{A_B(H_{BD})_B(T_D - T_B)}{\rho_G C_{pG} Q_B},$$

$$T_B = T_F \text{ at } h = 0 \quad (21a)$$

Let  $A_B(H_{BD})_B/\rho_G C_{pG} Q_B = \beta$ ; the temperature profile in the bubble phase be calculated by integrating Eq. (21a):

$$T_B = T_D - (T_D - T_F)e^{-\beta h} \quad (21b)$$

### 3.2.2. Mass and energy balances for the dense phase

The mass balance for components in the dense phase at steady state is given by

$$N_{iD} = N_{iDF} + \int_0^H (k_{EB})_{iB} \left[ \left( \frac{N_{iB}}{Q_B} \right) - \left( \frac{N_{iD}}{Q_D} \right) \right] + V(1 - \delta)(1 - \varepsilon)\rho_c R_i \quad (22)$$

Eq. (22) can be rearranged and the integral evaluated to give the molar flow rate of components in the dense phase. Substituting Eq. (20) into Eq. (22), and evaluating the integral of Eq. (22), then the molar flow rate of component  $i$  in the dense phase can be expressed by

$$N_{iD} = N_{iDF} + Q_B \left[ \left( \frac{N_{iF}}{Q_F} \right) - \left( \frac{N_{iD}}{Q_D} \right) \right] (1 - e^{-\alpha_i H}) + V(1 - \delta)(1 - \varepsilon)\rho_c R_i \quad (23)$$

The energy balance of the dense phase is given by

$$\begin{aligned} & \sum_{i=1}^{10} N_{iD} C_{p_{iD}} (T_D - T_{rf}) \\ &= \sum_{i=1}^{10} N_{iDF} C_{p_{iF}} (T_F - T_{rf}) \\ &+ \int_0^H (H_{BD})_B (T_B - T_D) A_B dh \\ &+ V(1 - \delta)(1 - \varepsilon)\rho_c \sum (-\Delta H_j r_j) \end{aligned} \quad (24)$$

Eq. (24) is rearranged and the integral evaluated (using Eq. (21b)) to give

$$\begin{aligned} & \sum_{i=1}^{10} N_{iD} C_{p_{iD}} (T_D - T_{rf}) \\ &= \sum_{i=1}^{10} N_{iDF} C_{p_{iF}} (T_F - T_{rf}) \\ &+ \rho_G C_{pG} Q_B (T_F - T_D)(1 - e^{-\beta H}) \\ &+ V(1 - \delta)(1 - \varepsilon)\rho_c \sum (-\Delta H_j r_j) \end{aligned} \quad (25)$$

The above equations provide the necessary mass and energy balances of the bubble and dense phases. The products of the two phases are then mixed at the bed exit to form the exit stream of the fluidized bed dehydrogenation reactor. The exit molar flow rates of the product components and temperature are given by

$$N_{iE} = N_{iD} + N_{iB} \quad (26)$$

$$T_E = \frac{T_D Q_D + T_B Q_B}{Q_D + Q_B} \quad (27)$$

The conversions and yields of reactants and products are calculated using the following equations for:

*Conversions:*

$$X_i = \frac{(N_{iF} - N_{iE})}{N_{iF}} \quad (28)$$

*Yields:*

$$Y_i = \frac{(N_{iE} - N_{iF})}{N_{(EB \text{ or } H_2O)F}} \quad (29)$$

### 3.2.3. Rate of hydrogen permeation through the palladium membrane

It is the same relation as for the fixed bed (Eq. (15)) and it is integrated along the length of the membrane, and the total hydrogen permeated is subtracted from the hydrogen balance.

## 3.3. Intrinsic kinetics for the industrial catalyst and in-house prepared catalysts

### 3.3.1. Intrinsic kinetics for the industrial catalyst

One set of industrial reactor data [1] is given in Table 1. The heterogeneous model, without the selective membranes, was used to extract the intrinsic kinetics from this set of industrial reactor data. An iteration procedure based on comparison between the industrial data and the heterogeneous model prediction was used till the iterations converged to the intrinsic parameters. After the intrinsic kinetic parameters were determined using this industrial set of data, the model was verified against other sets of industrial data without any adjustable parameters to insure the model power of predictability. Table 2 shows the heterogeneous model predictions using these intrinsic parameters as compared with the industrial data. Clearly the model simulates the industrial reactor very well.

Table 3  
Surface characteristics of the three in-house prepared catalysts

Catalyst	Density $\times 10^{-3}$ (kg/m <sup>3</sup> )	$S_{\text{BET}} \times 10^{-3}$ (m <sup>2</sup> /kg)	$V_p \times 10^3$ (m <sup>3</sup> /kg)	$r_p \times 10^9$ (m)
A <sup>a</sup>	4.541	15.333	0.1288	20.7
B <sup>b</sup>	4.920	28.426	0.1838	15.5
C <sup>c</sup>	4.939	34.112	0.1745	12.3

<sup>a</sup> Catalyst A 80%Fe<sub>2</sub>O<sub>3</sub>–20%K<sub>2</sub>O.

<sup>b</sup> Catalyst B 75%Fe<sub>2</sub>O<sub>3</sub>–20%K<sub>2</sub>O–5%CeO<sub>2</sub>.

<sup>c</sup> Catalyst C 70%Fe<sub>2</sub>O<sub>3</sub>–20%K<sub>2</sub>O–5%CeO<sub>2</sub>–5%Cr<sub>2</sub>O<sub>3</sub>.

### 3.4. Intrinsic kinetics for in-house prepared catalysts

#### 3.4.1. Preparation of the catalyst

The in-house catalysts were prepared by wet mixing iron oxide ( $\alpha$ -Fe<sub>2</sub>O<sub>3</sub>), potassium carbonate (K<sub>2</sub>CO<sub>3</sub>) and the corresponding amount of promoter in a rotary evaporator. Water was removed under vacuum at 70°C until a consistency of a flowable powder is obtained. The catalysts were dried at 120°C and calcined at 600°C overnight with air flowing at 100 ml/min. Three catalysts of different compositions were prepared — catalyst A: 80 wt.% Fe<sub>2</sub>O<sub>3</sub>–20 wt.% K<sub>2</sub>O (80Fe–20K), catalyst B: 75 wt.% Fe<sub>2</sub>O<sub>3</sub>–20 wt.% K<sub>2</sub>O–5 wt.% CeO<sub>2</sub> (75Fe–20K–5Ce) and catalyst C: 70 wt.% Fe<sub>2</sub>O<sub>3</sub>–20 wt.% K<sub>2</sub>O–5 wt.% CeO<sub>2</sub>–5 wt.% Cr<sub>2</sub>O<sub>3</sub> (70Fe–20K–5Ce–5Cr) (characteristics of the three catalysts are given in Table 3). The three catalysts differ considerably in composition from the industrial catalyst considered in this study which has the following composition: 62% Fe<sub>2</sub>O<sub>3</sub>, 36% K<sub>2</sub>CO<sub>3</sub> and 2% Cr<sub>2</sub>O<sub>3</sub> (62Fe–36K–2Cr).

#### 3.4.2. Reaction equipment and experimental procedure

A standard integral laboratory reactor using powdered catalyst with  $\eta = 1.0$  is used. A stream of helium at designated flow rate was metered through a steam generator while another line served as a carrier of feed as dispensed from a Masterflex liquid metering pump. A heating tape at 200°C placed before the reactor prevented condensation of the ethylbenzene. The catalyst bed is composed of a catalyst mixture (1.0 g catalyst/1.0 g ceramic) situated between two inert ceramic layers inside the 65 cm long and 0.75 cm ID stainless steel reactor tube. The reactor set-up is heated by a temperature-controlled tubular furnace. Products and unreacted reactants are passed through a condenser and sample condensates are collected for analysis.

Prior to the experimental determinations, the bed was first heated overnight at 600°C under a stream of air to remove contamination. Both feed and product were analyzed by a Varian Aerograph model 940 gas chromatograph using a flame ionization detector (FID). The column used was a 10 ft  $\times$   $\frac{1}{8}$  in. stainless steel tube packed with 20% DC-200 of Chromosorb W. The catalyst performance was expressed by the following formulae:

Ethylbenzene conversion,

$$\%C = \left( \frac{EB_{\text{inlet}} - EB_{\text{outlet}}}{EB_{\text{inlet}}} \right) 100$$

$$\text{Styrene selectivity, } \%S = \left( \frac{ST}{ST + BZ + TOL} \right) 100$$

Samples of the results for catalysts A–C are shown in Tables 4–6. Using the pseudo-homogeneous model and fitting the kinetic parameters to the experimental results, the values of the pre-exponential factors and activation energies that minimizes the mean square of the difference between the model predictions and the experimental results were obtained.

Table 7 gives the kinetic parameters for these catalysts, together with the kinetic parameters of the industrial catalyst obtained earlier. Also the equilibrium constant for the reversible ethylbenzene dehydrogenation reaction is given in the same table.

## 4. Results and discussion

Tables 8–11 show the results for different configurations, namely, the industrial fixed bed without membranes, the fixed bed with hydrogen selective membranes and the bubbling fluidized beds with and without membranes. For valid comparison between the four configurations, they are compared on the basis of similar design and operating parameters which are

Table 4

Feed conditions and experimental results of catalyst A

Temperature (°C)	He rate (ml/min)	Pressure (bar)	EB, %C	BZ, %S	TOL, %S	ST, %S
EB feed = 0.145 ml/min, H <sub>2</sub> O feed = 0.362 ml/min						
500	330	1.468	2.03	1.23	–	98.77
530	330	1.468	3.02	2.46	–	97.54
560	330	1.463	3.80	1.84	–	98.16
590	330	1.463	5.96	2.03	–	97.97
620	330	1.433	11.01	2.54	–	97.46
650	330	1.363	19.89	3.55	0.45	96.00
680	330	1.313	32.01	4.61	1.57	93.82
710	330	1.263	38.66	6.35	2.76	90.89
740	330	1.313	51.46	8.09	5.86	86.05

Table 5

Feed conditions and experimental results of catalyst B

Temperature (°C)	He rate (ml/min)	Pressure (bar)	EB, %C	BZ, %S	TOL, %S	ST, %S
EB feed = 0.139 ml/min, H <sub>2</sub> O feed = 0.3348 ml/min						
500	460	1.113	0.09	1.73	–	98.27
530	460	1.113	1.52	2.54	–	97.46
560	460	1.113	2.98	2.01	–	97.99
590	460	1.113	5.59	1.96	–	98.04
620	460	1.113	10.53	2.33	–	97.67
650	460	1.113	14.92	3.88	–	96.12
680	460	1.113	26.71	3.99	1.01	95.00
710	460	1.113	40.91	4.69	1.96	93.35
740	460	1.113	53.14	6.57	4.05	89.38

Table 6

Feed conditions and experimental results of catalyst C

Temperature (°C)	He rate (ml/min)	Pressure (bar)	EB, %C	BZ, %S	TOL, %S	ST, %S
EB feed = 0.1498 ml/min, H <sub>2</sub> O feed = 0.3348 ml/min						
502	450	1.624	9.07	2.23	– <sup>a</sup>	97.77
520	450	1.624	12.30	2.17	–	97.83
540	450	1.624	15.79	2.50	–	97.50
560	450	1.624	19.53	2.65	–	97.35
580	450	1.624	30.68	3.66	0.83	95.51
600	450	1.624	36.73	4.19	1.09	94.72
620	450	1.624	43.94	5.01	1.83	93.15
645	450	1.624	52.70	6.37	2.86	90.77
660	450	1.624	55.02	8.16	4.29	87.54
690	450	1.692	63.01	11.0	8.39	80.61
710	450	1.692	67.09	14.46	12.40	73.14
EB feed = 0.1595 ml/min, H <sub>2</sub> O feed = 0.3345 ml/min						
500	600	1.760	3.58	3.11	–	96.89
530	600	1.760	5.82	3.3	–	96.68
560	600	1.760	9.77	3.6	–	96.32
590	600	1.760	18.03	4.38	–	95.62
620	600	1.794	31.77	5.09	2.43	92.48

<sup>a</sup> Value was too small to be detected.

Table 7

Value of the kinetic parameters for the different catalysts ( $A_i$ : dimensionless pre-exponential factor,  $k_i = 3600 \exp(A_i - E_i/RT)$ ,  $E_i$ : activation energy)

Reaction	Industrial catalyst		Catalyst A		Catalyst B		Catalyst C	
	$A_i$	$E_i$	$A_i$	$E_i$	$A_i$	$E_i$	$A_i$	$E_i$
1	0.851	90891	0.30	87820	0.43	86565	0.75	83357
2	14.00	207989	13.25	193515	13.35	187992	12.19	188630
3	0.56	91515	−0.38	102668	0.81	97334	0.77	100555
4	0.12	103996	0.12	103996	0.12	103996	0.12	103996
5	−3.21	65723	−3.21	65723	−3.21	65723	−3.21	65723
6	21.24	73628	21.24	73628	21.24	73628	21.24	73628

Equilibrium constant  $K_{EB} = \exp(-\Delta F_0/RT)$  (bar), [19]:  $\Delta F_0 = a + bT + cT^*$

\*  $a = 122725.157$  (kJ/kmol);  $b = -126.2674$  (kJ/kmol K);  $c = -2.194 \times 10^{-3}$  (kJ/kmol K<sup>2</sup>).

Table 8

Results of the industrial catalyst

Components	Fixed bed	Fixed bed with membrane	Fluidized bed	Fluidized bed with membrane
<i>Conversion (%)</i>				
Ethylbenzene	47.47	53.16	36.05	69.11
<i>Yield (%)</i>				
Styrene	40.17	49.17	20.72	65.33
Benzene	4.12	3.50	4.03	3.68
Toluene	3.17	0.64	11.31	0.01

Table 9

Results of in-house catalyst A

Components	Fixed bed	Fixed bed with membrane	Fluidized bed	Fluidized bed with membrane
<i>Conversion (%)</i>				
Ethylbenzene	46.49	52.57	34.16	67.88
<i>Yield (%)</i>				
Styrene	33.02	41.3	19.54	55.56
Benzene	13.15	11.20	13.79	12.17
Toluene	0.32	0.01	0.83	0.15

Table 10

Results of in-house catalyst B

Components	Fixed bed	Fixed bed with membrane	Fluidized bed	Fluidized bed with membranes
<i>Conversion (%)</i>				
Ethylbenzene	52.35	58.25	37.74	73.49
<i>Yield (%)</i>				
Styrene	28.36	39.25	12.72	54.00
Benzene	22.09	18.57	19.54	19.41
Toluene	1.89	0.43	5.49	0.08

Table 11  
Results of in-house catalyst C

Components	Fixed bed	Fixed bed with membrane	Fluidized bed	Fluidized bed with membranes
<i>Conversion (%)</i>				
Ethylbenzene	51.27	64.84	36.29	79.05
<i>Yield (%)</i>				
Styrene	44.28	60.51	23.42	75.36
Benzene	5.97	4.15	9.13	3.67
Toluene	1.01	0.17	3.74	0.02

the same as those of the industrial fixed bed reactor. For the fluidized bed configurations, the same amount of catalyst is used. However, for the same amount of catalyst different other parameters affect the operation such as the height to diameter ratio as well as powder particle size. These parameters affect the hydrodynamic characteristics and thus the performance of the fluidized bed reactor. In this paper a value of  $H/D$  of 0.873 and  $d_p$  of 0.363 mm (363  $\mu\text{m}$ ) are used. This particle size belongs to group B ( $d_p = 40\text{--}500\ \mu\text{m}$ ) according to the classification of Geldart [20,21].

For the two types of membrane reactors, the same type of membrane is used with the same total permeation surface area. The composite membranes used are formed of thin palladium layer  $5.0 \times 10^{-4}$  mm in thickness supported on porous ceramic tubes with a diameter of 6.87 cm. The number of membrane tubes used is 30, the sweep gas molar flow rate is 750 kmol/h. The pressure in the sweep gas side is 1.013 bar and in the reactor side is 2.0 bar. Heat transfer through the membrane was neglected in the present investigation because of the low thermal conductivity of the ceramic composite membranes used. It is clear from the tables that for all four catalysts the use of membranes causes the following:

1. Increase in ethylbenzene (EB) conversion and styrene (ST) yield due to the enhancement of the styrene formation forward reaction associated with the removal of hydrogen.
2. Decrease of toluene yield due to suppression of the hydrogenation reaction associated with hydrogen removal.
3. Decrease in benzene formation because of the enhancement of the ethylbenzene to styrene reaction associated with hydrogen removal.

#### 4.1. The industrial fixed bed reactor without membranes

It is clear from Tables 8–11 that for the industrial fixed bed configuration, the best catalyst for the production of styrene is catalyst C. The EB conversion using catalyst C is 8% higher than the industrial catalyst whereas the styrene yield is 10.2% higher. The yield of benzene is 4.5% higher and toluene 2.14% higher. It is interesting to notice that the catalyst with the highest activity (EB % conversion) which is catalyst B, produces the lowest styrene yield. For this catalyst, although EB conversion is 10.3% higher than the industrial catalyst, the styrene yield is 28.73% lower. The loss in styrene yield associated with the most active catalyst is due to the large production of benzene. According to the reaction mechanism, benzene is not a secondary product that can be decreased through a decrease in residence time. It is actually a primary product resulting from competition between the two parallel reactions: EB to styrene and EB to benzene. The benzene yield for catalyst B is 436.16% higher than that for the industrial catalyst. Based on simulation results in Tables 8–11, the catalysts can be graded for the fixed bed configuration without membranes as shown in Table 12. Based on activity (EB conversion) and selectivity (styrene yield, ST.Y), the most active catalyst is catalyst B, while the most selective catalyst is catalyst C.

#### 4.2. Fixed bed reactor with hydrogen selective membranes

It is clear that the use of composite hydrogen selective membrane increases the EB conversion and styrene yield for all catalysts in different degrees, e.g.

Table 12

Grading of the different catalysts for the different configurations (ind.=industrial catalyst, AC=activity, St.Y=styrene yield, A, B, C=the three in-house prepared catalyst)

Grading	CONF 1 <sup>a</sup>		CONF 2 <sup>b</sup>		CONF 3 <sup>c</sup>		CONF 4 <sup>d</sup>	
	AC	ST.Y	AC	ST.Y	AC	ST.Y	AC	ST.Y
No. 1	B	C	C	C	B	C	C	C
No. 2	C	Ind.	B	Ind.	C	Ind.	B	Ind.
No. 3	Ind.	A	Ind.	A	Ind.	A	Ind.	A
No. 4	A	B	A	B	A	B	A	B

<sup>a</sup> CONF 1 = configuration 1 = fixed bed reactor.

<sup>b</sup> CONF 2 = configuration 2 = fixed bed reactor with hydrogen selective membranes.

<sup>c</sup> CONF 3 = configuration 3 = fluidized bed reactor.

<sup>d</sup> CONF 4 = configuration 4 = fluidized bed reactor with hydrogen selective membrane.

EB conversion and styrene yield for the industrial catalyst increase by 12 and 22.4%, respectively, while for catalyst C, the corresponding percentage increases are 26.6 and 36.6%. For the fixed bed configuration with composite hydrogen selective membrane, catalyst C is the best catalyst for both activity and styrene yield. An important effect is noticed for catalyst A which, although the least active catalyst, gives higher styrene yield than catalyst B. Table 12 shows the grading of the four catalysts with respect to both activity (AC) and styrene yield (ST.Y) for the fixed bed configuration with selective membranes.

#### 4.3. Fluidized bed reactor without membranes

It is clear from Tables 8–11 that for the fluidized bed without composite hydrogen selective membranes, a dramatic drop in EB conversion and styrene yield occurs as compared to the fixed bed without membranes, e.g. for the industrial catalyst the drop in EB conversion and styrene yield is 24.05 and 48.4 %, respectively, while for catalyst C it is 29.2 and 47.1%.

This result is in contradistinction to our earlier modeling and pilot plant results for the steam reforming of natural gas [16,17] which showed a considerable improvement in conversion and hydrogen yield through the use of the fluidized bed configuration with and without hydrogen selective membranes. The considerable improvements in the performance of the fluidized steam reforming without membranes are due to two factors which are the following:

1. The very large increase in the effectiveness factor,  $\eta$  since  $\eta$  in fixed bed steam reformers is in the

range of  $10^{-2}$ – $10^{-3}$  [18] due to the very strong diffusional limitations.

2. The small molecules involved in the reaction and their high mass transfer coefficient for diffusion between the bubble and dense phases, thus minimizing the negative effect of reactants by-pass through the bubbles.

The situation with the EB dehydrogenation system is different as follows:

1. The effect of diffusional limitations is not as strong as for the fixed bed steam reformer ( $\eta$  for the EB to styrene reaction is in the range 0.6–0.8).
2. The effect of reactants by-pass through the bubbles, is strong because of the large molecules involved and consequently the large diffusional resistances between the bubble and the dense phases for almost all molecules involved except hydrogen.

It is clear from Table 12 that for this configuration, catalyst C is the best with regard to the styrene yield but is second best (after catalyst B) with respect to activity.

#### 4.4. Fluidized bed reactor with hydrogen selective membranes

As shown in Tables 8–11, a very large increase in EB conversion and styrene yield for all catalysts is observed when hydrogen selective membranes are used with the fluidized bed configuration. This is mostly due to the mixing in the fluidized bed which achieves a much higher utilization of the membranes for hydrogen removal than in fixed bed, where part of the

membranes is exposed to low hydrogen concentration at the entrance part of the fixed bed.

For fixed beds, in the case of catalyst A the use of selective membranes increases EB conversion (in comparison with fixed bed without membranes) from 47.47 to 53.16% which represents a 12% increase. As for styrene yield, the increase is from 40.17 to 49.17%, which represents a 22.4 % increase. For the same catalyst A in the fluidized bed, the use of hydrogen selective membranes increases EB conversion from 36.05 to 69.11% which represents a 91.7% increase and for styrene yield the increase is 215.3% (from 20.72 to 65.33%).

For catalyst C, the same comparison reveals that the increase in activity due to the use of selective membranes in fixed beds is from 51.27 to 64.84% which represents a 26.5% increase. With respect to styrene yield, the increase is from 44.28 to 60.51% (35.8% increase). In fluidized beds EB conversion increases from 36.29 to 79.05%, an increase of 117.8%. Styrene yield increases from 23.42 to 75.36%, an increase of 212.7%.

The grading of the catalysts for this fluidized bed with a hydrogen selective membrane configuration is shown in Table 12.

## 5. Conclusions

The presented procedure of integrating the kinetic and reactor modeling for catalytic processes gives deeper and more quantitative insight into the behavior of each catalyst in each reactor configuration. It also allows the evaluation of the performance of the different catalysts when used in some novel configurations such as fixed beds with membranes and fluidized beds with/without membranes.

The rigorous heterogeneous model for the classical industrial fixed bed configuration allows the extraction of intrinsic kinetic parameters from industrial data. This facilitates the systematic comparison of the industrial catalysts for the different suggested configurations.

Rigorous, reliable reactor models integrated with reliable kinetic data and kinetic models are very powerful tools in the development of a process from

the laboratory scale to the commercial scale. These models can help to save the expensive pilot plant stage or at least minimize its cost and maximize its utilization.

Work is underway to develop object-oriented user friendly software package where the user can simply introduce the results of the experimental laboratory scale measurements, the suggested mechanism and functional form of the kinetic rate equation and obtain the kinetic parameters for the different catalysts and the performance of each catalyst in a number of membrane/non-membrane configurations.

## References

- [1] G.J.P. Sheel, C.M. Crowe, *Can. J. Chem. Eng.* 47 (1969) 183.
- [2] D.E. Clough, W.F. Ramirez, *AIChE J.* 22 (1976) 1097.
- [3] R. Aris, *Chem. Eng. Sci.* 6 (1957) 262.
- [4] E.A. Mason, A.P. Malinaukas, R.B. Evans, *J. Chem. Phys.* 46 (1967) 3199.
- [5] S.S.E.H. Elnashaie, M.E.E. Abashar, *Latin Am. Appl. Res.* 23 (1992) 89.
- [6] S.S.E.H. Elnashaie, S.S. Elshishini, *Modeling, Simulation and Optimization of Industrial Fixed Bed Catalytic*, Gordon and Breach, UK, 1994.
- [7] J. Villadsen, M.L. Michelsen, *Solution of Differential Equation Models by Polynomial Approximation*, Prentice-Hall, New York, 1987.
- [8] J. Villadsen, W.E. Stewart, *Chem. Eng. Sci.* 22 (1967) 1483.
- [9] R.B. Bird, W.E. Stewart, E.N. Lightfoot, *Transport Phenomena*, Wiley, New York, 1960.
- [10] G. Bohmholdt, Wicke, *Z. Physik. Chem. N.F.* 56 (1967) 133.
- [11] T.T.N. Tsotsis, N. Nourbarkhsh, I.A. Webster, *Am. Chem. Soc., Div. Petr. Chem. Prepr.* 33 (1989) 502.
- [12] J.R. Grace, NATO, ASI Ser., Ser. E., Vol. 110, *Chem. Reactor Design Technology*, 1986, p. 245.
- [13] S. Mori, C.Y. Wen, *AIChE J.* 21 (1975) 109.
- [14] D. Kunii, O. Levenspiel, *Fluidization Engineering*, Wiley, New York, 1969.
- [15] R.C. Reid, T.K. Sherwood, *The Properties of Gases and Liquids*, McGraw-Hill, New York, 1966.
- [16] A.M. Adris, S.S.E.H. Elnashaie, R. Hughes, *Can. J. Chem. Eng.* 69 (1991) 1061.
- [17] A.M. Adris, J.R. Grace, C.J. Lim, S.S.E.H. Elnashaie, *US Patent No.* 5,326,550 (1994).
- [18] M.A. Soliman, S.S.E.H. Elnashaie, A.S. Al-Ubaid, A.M. Adris, *Chem. Eng. Sci.* 43 (1988) 1801.
- [19] R.H. Boundy, R.F. Boyer, *Styrene, its Polymers, Copolymers and Derivatives*, Reinhold, New York, 1952.
- [20] J. Visser, *Powder Technol.* 58 (1989) 1.
- [21] D. Geldart, *Powder Technol.* 6 (1972) 201.